Berry phase modification of the current drive in a restricted class of large annular Josephson junctions at low temperature

Frank Gaitan*
Department of Physics, Southern Illinois University, Carbondale, Illinois 62901-4401
(Received 10 May 2000; revised manuscript received 28 July 2000; published 20 February 2001)

We examine how Berry's phase influences the motion of vortices in a restricted class of large annular Josephson junctions at sufficiently low temperatures. We show that the essential physical effect produced is a modulation of the tunnel current density passing through the junction which, however, leaves the total current through the junction unaffected. The tunnel current density modulation is seen to produce a spatially inhomogeneous modification of the current drive which acts on a vortex residing in an annular junction of this restricted type. We discuss the circumstances under which this current drive modification vanishes, and provide an estimate of the temperature at which its effects will be masked by spectral flow.

DOI: 10.1103/PhysRevB.63.104511 PACS number(s): 74.50.+r, 03.65.Ta, 74.60.−w

I. INTRODUCTION

Previously,[1] it has been argued that Berry's phase[2] will influence the motion of vortices in a large annular Josephson junction at $T=0$. In this paper, we provide the details of that argument, and discuss the conditions under which this Berry phase effect is expected to be observable. We will see that two restrictions are essential for an observable effect. The first is that the electron dynamics is in the collisionless limit so that spectral flow[3–6] will not mask the Berry phase effect which is the focus of this paper. The second requires that the annular Josephson junction belong to a restricted class which we define explicitly later in this paper.

For a current-biased annular Josephson junction (AJJ) satisfying the above restrictions, we will see that Berry's phase causes a modulation of the tunnel current density.[7] It is worth noting, however, that the total tunnel current through the junction is uneffected, and remains equal to the bias current fed into the junction. Formally, the manifestation of the tunnel current density modulation is a spatially inhomogeneous modification of the current drive acting on a vortex in the junction. Examination of the explicit form of the current drive modification shows that it vanishes identically for a traditional linear Josephson junction, as well as for the well-known Lyngby AJJ. We provide two examples of AJJ's for which the current drive modification does not vanish.

To ensure that the electron dynamics is in the collisionless limit, we specifically require that (1) the electrodes and weak link that make up the AJJ be in the clean limit, (2) the weak link have uniform thickness, and (3) the temperature be sufficiently low as to rule out activation of spectral flow via thermal effects. We provide a more quantitative discussion of condition (3) later in this paper.

The structure of our presentation is as follows. In Sec. II we demonstrate how Berry's phase causes a modulation of the tunnel current density passing through a current-biased AJJ,[7] and how this modulation in turn produces a modification of the current drive acting on a vortex in the junction. Section III examines the conditions under which the current drive modification is expected to be observable. This discussion explicitly defines the restricted class of AJJ's for which the current drive modification does not trivially vanish, as well as elaborating on the conditions needed to ensure the absence of spectral flow. Section IV provides a summary of the essential results found, while in the Appendix, we provide a brief review of how Berry's phase influences the motion of the superconducting electrons present in the electrodes that feed current into the AJJ. It is this Berry phase effect which ultimately causes the current drive modification discussed in Sec. II.

II. BERRY'S PHASE AND THE CURRENT DRIVE AT $T=0$

In a Josephson junction, two superconducting electrodes are coupled through a weak link which often is either (i) a normal metallic layer that separates the superconducting electrodes (SNS junction) or (ii) an insulating layer which provides the separation (SIS junction). This coupling of the superconductivity of disjoint superconductors across a weak link originates in an interaction energy between the superconductors which is sensitive to the difference in values of the gap phases of each superconductor, $\gamma=\gamma_1-\gamma_2$. The difference in phase values γ is known as the Josephson phase and it is the sole low-energy degree of freedom of the junction. γ is highly sensitive to magnetic fields, resulting in screening effects which occur on a length scale λ_J known as the Josephson penetration length. Junctions whose weak link has a transverse length $L\gg\lambda_J$ are referred to as large Josephson junctions. In a large Josephson junction magnetic flux can penetrate into the weak link in localized regions known as fluxons or vortices. In this paper we restrict ourselves to large annular Josephson junctions in which the weak link has an annular geometry.

It is well known[8] that the dynamics of an isolated ideal large Josephson junction is governed by the sine-Gordon equation

$$\frac{\partial^2\gamma}{\partial\tau^2}-\nabla_\perp^2\gamma+\sin\gamma=0. \tag{1}$$

Here (1) $\tau=\omega_J t$ is the dimensionless time measured in units of the inverse Josephson plasma frequency ω_J^{-1}, (2) the position along the surface of the weak link is parametrized by

the dimensionless coordinate $\mathbf{l}_\perp = \mathbf{x}_\perp / \lambda_J$, and (3) $\nabla_\perp$ is the gradient operator with respect to $\mathbf{l}_\perp$. It is important to note that this equation applies to all types of isolated ideal large Josephson junctions (SNS, SIS, etc.). In fact, as Josephson showed, the necessary ingredients for its derivation are Ampère's law, together with the fundamental Josephson relations

$$\frac{\hbar \omega_J}{2e} \frac{\partial \gamma}{\partial \tau} = V, \quad \frac{1}{\lambda_J} \nabla_\perp \gamma = \frac{2ed}{\hbar c} \mathbf{H} \times \hat{\mathbf{n}}. \tag{2}$$

Equations (2) express the fundamental sensitivity of γ to voltage V and magnetic field $\mathbf{H}$. Here d is the magnetic thickness of the weak link, and $\hat{\mathbf{n}}$ points across the weak link from one superconducting electrode to the other, and consequently is orthogonal to $\mathbf{l}_\perp$. Equation (1) can be obtained variationally from the sine-Gordon action S_0:

$$S_0 = \int d\tau \, d^2 l_\perp \left[\frac{1}{2} \left(\frac{\partial \gamma}{\partial \tau} \right)^2 - \frac{1}{2} (\nabla_\perp \gamma)^2 - (1 - \cos \gamma) \right]. \tag{3}$$

In reality, one never encounters an isolated ideal Josephson junction. For a real junction, the dynamics of Eq. (1) will be modified by a number of physical effects.[9,10] The first modification is due to nonuniformity in the thickness of the weak link arising from imperfections in the fabrication process. To simplify the analysis below, we assume that junction fabrication was done with sufficient care that this type of modification is small and can be ignored or, if necessary, treated perturbatively. Thus we explicitly restrict ourselves to clean weak links of uniform thickness. The second type of modification is caused by dissipative processes occurring in the junction. Dissipation arises from normal currents passing through the weak link and from normal currents which flow at the surface of the electrodes transverse to the weak link. These effects occur at finite temperature and their contributions to Eq. (1) will be included later in this section. The final type of modification we consider arises when we connect the junction to a current source. This drives a bias current through the weak link which accelerates any vortices present within the link. The bias current contributes a driving term to Eq. (1) which is known as the current drive. In this section we will show that for a clean AJJ of uniform thickness at $T=0$ the current drive includes a Berry-phase-induced modification. It will be clear from the derivation that the current drive modification will appear in both SNS and SIS AJJ's. In Sec. III we will see that further restrictions are necessary if the current drive modification is to be observable at nonzero temperature.

A. Current density modification

Before we begin our discussion of the current drive, it would be useful to describe the AJJ in a bit more detail. We have in mind a planar AJJ as shown in Fig. 1. Superconductor 1 (denoted SC1) corresponds to a circular disk of superconducting material of radius R_1. Superconductor 2 (SC2) is a superconducting film in which a circular region of radius $R_2 \gtrsim R_1$ has been removed. The AJJ is formed by placing SC1 concentrically inside the circular hole in SC2.

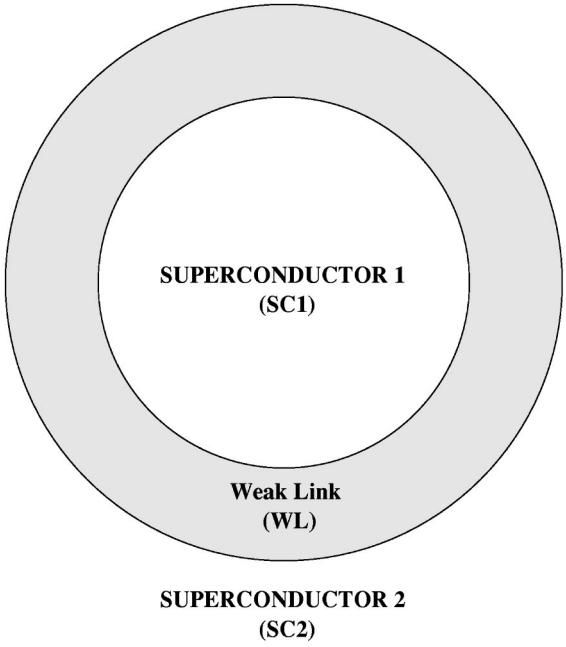

FIG. 1. Top view of a planar annular Josephson junction. See Sec. II A for further discussion.

The weak link (WL) corresponds to the annular region separating SC1 from SC2 with a thickness $\Delta R = R_2 - R_1 \ll R_1$.

To simplify things, we consider an AJJ of height λ_J. We introduce polar coordinates (r, θ) with origin at the common center of SC1 and SC2. We parametrize position $\mathbf{l}_\perp$ along the annular weak link in terms of height z and arc length $s = \bar{R}\theta$, where $\bar{R} = (R_1 + R_2)/2$. In Fig. 2 we show a portion of the AJJ which details our coordinate system.

For the remainder of this paper we will assume that a bias current I is passed through the AJJ. Because we assume a weak link of uniform thickness, the bias current density $\mathbf{j}_T = j_T \hat{\mathbf{j}}_T$ flows radially through the weak link so that $\hat{\mathbf{j}}_T = \pm \hat{\mathbf{r}}$, and its magnitude $j_T \equiv \rho_s |e| v_T$ is independent of position s along the link. We further assume that a single vortex is present in the weak link with magnetic flux pointing along $\hat{\mathbf{z}}$. A vortex is shown in Fig. 2 together with a schematic representation of the associated screening currents. The screening currents penetrate into the two superconductors to a distance of order λ (penetration length), and go to zero as one moves away from the region of localized magnetic flux (vortex core). Under these circumstances the superflow in superconductor i $(i=1,2)$ is $\mathbf{v}_s(i) = \mathbf{v}_T + \mathbf{v}_{circ}(i)$. Here $\mathbf{v}_T$ is the superflow velocity associated with $\mathbf{j}_T$, and $\mathbf{v}_{circ}(i) = (\hbar/2m) \nabla \gamma_i$ is the superflow velocity associated with the portion of the screening currents that flow inside superconductor i.

In a traditional linear Josephson junction (LJJ) the bias current I produces a driving term $\beta = I/I_c$ known as the current drive in the sine-Gordon equation [Eq. (1)]:

$$\frac{\partial^2 \gamma}{\partial \tau^2} - \nabla_\perp^2 \gamma + \sin \gamma = \pm \beta. \tag{4}$$

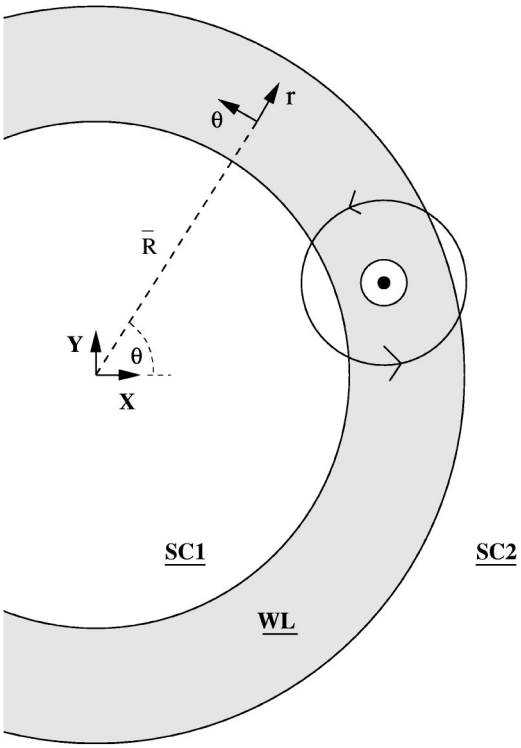

FIG. 2. Coordinate system for a planar annular Josephson junction containing a single vortex with magnetic flux along $\hat{\mathbf{z}}$. The closed loop is a schematic representation of the screening currents circulating around the vortex center.

The choice of sign on the right-hand side (RHS) corresponds to the two directions in which current can pass through the weak link $\hat{\mathbf{j}}_T = \pm \hat{\mathbf{n}}$, and I_c is the critical current for the AJJ. This equation of motion can be obtained variationally from the action

$$S_\gamma = \int d\tau\, d^2 l_\perp \left[\frac{1}{2}(\partial_\tau \gamma)^2 - \frac{1}{2}(\nabla_\perp \gamma)^2 - (1-\cos\gamma) \pm \beta\gamma \right]. \tag{5}$$

Note that, because the magnetic flux is assumed to point along $\hat{\mathbf{z}}$, it follows from Eq. (2) that the Josephson phase $\gamma = \gamma(l,\tau)$ only depends on $l = s/\lambda_J$ and $\tau = \omega_J t$, and is independent of height z. Thus $(\nabla_\perp \gamma)^2 = (\partial\gamma/\partial l)^2$, and the integration over height simply gives the assumed height λ_J.

It is clear that the $\beta\gamma$ term within the square brackets in Eq. (5) produces the current drive in Eq. (4). This contribution to S_γ can be derived from the microscopic action for our system of two superconductors coupled through a weak link:

$$S_{micro} = S_1 + S_2 + S_{int}. \tag{6}$$

Here S_i $(i=1,2)$ is the BCS action for the ith superconductor [see Eq. (A6) in the Appendix], and S_{int} describes the Josephson and capacitive coupling of the two superconductors across the weak link. We will now carry out the microscopic derivation of the current drive contribution to S_γ, and will show that β receives a Berry-phase-induced correction $\delta\beta$. This correction vanishes identically for a linear Josephson junction [so that we recover the familiar $\beta\gamma$ term in Eq. (5)], but is nonvanishing for a restricted class of AJJ's to be defined in Sec. III. The current drive modification $\delta\beta$ will be seen to be the consequence of a modulation of the tunnel current density flowing through the weak link caused by Berry's phase.[7] We will see, however, that the total current through the weak link is unaffected, and remains equal to the bias current I fed into the junction.

As discussed in the Appendix, the terms in S_{micro} responsible for producing the driving force on a vortex in the weak link originate in the actions S_i $(i=1,2)$ and are the terms which are linear in $\nabla_{\mathbf{r}}\gamma_i$ [see Eq. (A7)]:

$$S_{dr}(i) = \int dt\, d^3 x_i \left(-\frac{\hbar}{2e} \right) (\mathbf{j}_T + \Delta\mathbf{j}_B) \cdot \nabla_{\mathbf{r}} \gamma_i. \tag{7}$$

Here $\Delta\mathbf{j}_B = -\rho_s e \dot{\mathbf{r}}_0(t)$, and it is shown in the Appendix to be a consequence of Berry's phase. Using an identity from vector calculus, we can rewrite $S_{dr}(i)$ as

$$S_{dr}(i) = \int dt\, d^3 x_i \left(-\frac{\hbar}{2e} \right) \times [\nabla_{\mathbf{r}} \cdot \{\gamma_i (\mathbf{j}_T + \Delta\mathbf{j}_B)\} - \gamma_i \nabla_{\mathbf{r}} \cdot (\mathbf{j}_T + \Delta\mathbf{j}_B)]. \tag{8}$$

The second term in the integrand acts locally and is restricted to the interior of superconductor i. Consequently, it does not influence the dynamics of the Josephson phase $\gamma = \gamma_1 - \gamma_2$ which is determined by interactions at the superconductor boundaries which are adjacent to the weak link. The first term, however, converts into a boundary term $S_{bt}(i)$ through the divergence theorem and thus will influence the dynamics of γ:

$$S_{bt}(i) = \int dt\, d^2 x_\perp \left(-\frac{\hbar}{2e} \right) \{\gamma_i (\mathbf{j}_T + \Delta\mathbf{j}_B)\} \cdot \hat{\mathbf{n}}_i(s). \tag{9}$$

Here $\hat{\mathbf{n}}_i(s)$ is the outward normal to superconductor i at position $s = \bar{R}\theta$ along the annular weak link. From Fig. 2, $\hat{\mathbf{n}}_1(s) = -\hat{\mathbf{n}}_2(s) = \hat{\mathbf{r}}(s)$. It is clear from the derivation that the current density $\mathbf{j} = \mathbf{j}_T + \Delta\mathbf{j}_B$ appearing in Eq. (9) flows at the boundary surface of superconductor i. Its projection along the normal $\hat{\mathbf{n}}_i(s)$ gives the tunnel current density (to within a sign), while its component along the tangent plane contributes to the supercurrent flowing parallel to superconductor i's surface. This contribution to the surface supercurrent originates in $\Delta\mathbf{j}_B$ which has both a normal and a surface component (see Sec. II C). Note, however, that only the normal component of $\mathbf{j}$ exits the electrode and enters the weak link.

The current drive action $\overline{S_{cd}}$ is the sum of the boundary terms $S_{bt}(i)$:

$$\overline{S_{cd}} = S_{bt}(1) + S_{bt}(2)$$
$$= \int dt\, d^2x_\perp \left[\left(-\frac{\hbar}{2e} \right) (\mathbf{j}_T + \Delta\mathbf{j}_B) \cdot \hat{\mathbf{r}}(s) \right] (\gamma_1 - \gamma_2)$$
$$= \int dt\, d^2x_\perp \left(-\frac{\hbar}{2e} \right) [(\mathbf{j}_T + \Delta\mathbf{j}_B) \cdot \hat{\mathbf{r}}(s)]\, \gamma. \tag{10}$$

It is clear from the final line in Eq. (10) that the vortex drive is produced by the normal component of $\mathbf{j}$, and that this normal component receives a Berry-phase-induced contribution $\Delta\mathbf{j}_B \cdot \hat{\mathbf{r}}(s)$. It is important to note that the flux of $\Delta\mathbf{j}_B$ through the weak link vanishes:

$$\Delta I_B = \int_0^{\lambda_J} dz \int_0^{2\pi} \overline{R}\, d\theta [\Delta\mathbf{j}_B \cdot \hat{\mathbf{r}}(\theta)]$$
$$= -\lambda_J \overline{R} (\rho_s e \dot{\mathbf{r}}_0) \cdot \int_0^{2\pi} d\theta\, \hat{\mathbf{r}}(\theta) = 0. \tag{11}$$

Thus the total current flowing through the weak link remains equal to the bias current I as it should. From Eq. (11), we see that the Berry phase contribution to the tunnel current density, $\Delta\mathbf{j}_B \cdot \hat{\mathbf{r}}(s)$, is simply a spatial modulation of $\mathbf{j}_T$, enhancing it in one region by reducing it in another (see Sec. II C for further discussion).

B. Current drive modification

We now show how the component of $\Delta\mathbf{j}_B$ along $\hat{\mathbf{r}}(s)$ produces a modification of the current drive acting on a vortex in the weak link.

We begin by extracting the dimensionful quantities on which $\overline{S_{cd}}$ depends. Recalling that $\mathbf{j}_T = j_T \hat{\mathbf{j}}_T$, $j_T = \rho_s |e| v_T$, and $\Delta\mathbf{j}_B = -\rho_s e \dot{\mathbf{r}}_0$, it follows that

$$\overline{S_{cd}} = \int dt\, d^2x_\perp \left(\frac{\hbar J_c}{2|e|} \right) \left[\frac{j_T}{J_c} \left(\hat{\mathbf{j}}_T + \frac{\dot{\mathbf{r}}_0}{v_T} \right) \cdot \hat{\mathbf{r}}(s) \right] \gamma$$
$$= \left(\frac{E_J \lambda_J^2}{\omega_J} \right) \int d\tau\, d^2l_\perp \left[\beta\gamma \left(\hat{\mathbf{j}}_T + \frac{\dot{\mathbf{r}}_0}{v_T} \right) \cdot \hat{\mathbf{r}}(l) \right]. \tag{12}$$

Here $E_J = \hbar J_c / 2|e|$ is the Josephson coupling energy per unit area, J_c is the critical current density of the AJJ, and we note that $\beta = I/I_c = j_T/J_c$. The integral on the final line is the dimensionless current drive action S_{cd}. Noting that $\hat{\mathbf{j}}_T(l) = \pm \hat{\mathbf{r}}(l)$ since the bias current can flow through the weak link in either of two directions, we have that

$$S_{cd} = \int d\tau\, d^2l_\perp \left[\pm\beta\gamma \left(1 + \frac{\dot{\mathbf{r}}_0 \cdot \hat{\mathbf{j}}_T}{v_T} \right) \right]. \tag{13}$$

The second term in the integrand is due to the Berry phase modification $\Delta\mathbf{j}_B$ in Eq. (10). For a LJJ, $\hat{\mathbf{j}}_T$ is always orthogonal to $\dot{\mathbf{r}}_0$ (see Sec. III for a further discussion). Consequently, the Berry phase contribution to S_{cd} vanishes identically and S_{cd} reduces to the $\beta\gamma$ term in Eq. (5) as it should. However, the Berry phase term in S_{cd} does not vanish for a restricted class of AJJ's which will be defined in Sec. III. For this class of AJJ's, the junction action S_γ includes both contributions to S_{cd},

$$S_\gamma = \int d\tau\, d^2l_\perp \left[\frac{1}{2} \left(\frac{\partial\gamma}{\partial\tau} \right)^2 - \frac{1}{2} (\nabla_\perp \gamma)^2 - (1 - \cos\gamma) \right.$$
$$\left. \pm \beta\gamma \left(1 + \frac{\dot{\mathbf{r}}_0 \cdot \hat{\mathbf{j}}_T}{v_T} \right) \right], \tag{14}$$

and the equation of motion is

$$\frac{\partial^2\gamma}{\partial\tau^2} - \frac{\partial^2\gamma}{\partial l^2} + \sin\gamma = \pm[\beta + \delta\beta(l,\tau)]. \tag{15}$$

[Recall that $\gamma = \gamma(l,\tau)$ since the magnetic flux is assumed to point along $\hat{\mathbf{z}}$.] The sign choice on the RHS corresponds to $\hat{\mathbf{j}}_T(l) = \pm \hat{\mathbf{r}}(l)$. We see that the current drive includes the spatially inhomogeneous modification $\delta\beta(l,\tau)$ which is a consequence of the current density modification $\Delta\mathbf{j}_B$ produced by Berry's phase:

$$\delta\beta(l,\tau) = \frac{\beta}{v_T} \dot{\mathbf{r}}_0(\tau) \cdot \hat{\mathbf{j}}_T(l) = \hat{\mathbf{j}}_T(l) \cdot \frac{\Delta\mathbf{j}_B}{J_c}. \tag{16}$$

Since $\hat{\mathbf{j}}_T(l)$ is always normal to the local junction plane, we see that it is the component of $\Delta\mathbf{j}_B$ along $\hat{\mathbf{r}}(l)$ which is responsible for the current drive modification $\delta\beta(l,\tau)$ as already anticipated in Sec. II A. Note that our derivation of $\delta\beta$ made no assumptions about whether the AJJ is SNS or SIS. Consequently, the derivation applies to both cases. As will be discussed more fully in Sec. III, a class of AJJ's can be defined for which the scalar product appearing in $\delta\beta$ does not vanish. There we will discuss more fully the conditions needed for $\delta\beta$ to be observable in this restricted class of AJJ's at finite temperature.

Equation (15) determines the dynamics of a restricted class of AJJ's at $T = 0$ (see Sec. III, and recall that $\Delta\mathbf{j}_B$ was determined at $T = 0$ in the Appendix). At finite temperature, dissipation and spectral flow will act to modify the dynamics of this equation. Dissipation is produced by normal currents which (a) pass through the weak link or (b) flow at the surface of the superconducting electrodes parallel to the weak link.[9,10] As will be discussed in Sec. III, spectral flow is not active at sufficiently low temperatures. Thus, for such low temperatures, only dissipation modifies the dynamics of Eq. (15):

$$\frac{\partial^2\gamma}{\partial\tau^2} - \frac{\partial^2\gamma}{\partial l^2} + \sin\gamma = \pm[\beta + \delta\beta(l,\tau)] - a\frac{\partial\gamma}{\partial\tau} + b\frac{\partial^3\gamma}{\partial l^2 \partial\tau}. \tag{17}$$

Here dissipation due to normal currents flowing through (parallel to) the weak link produces the a (b) term on the RHS.

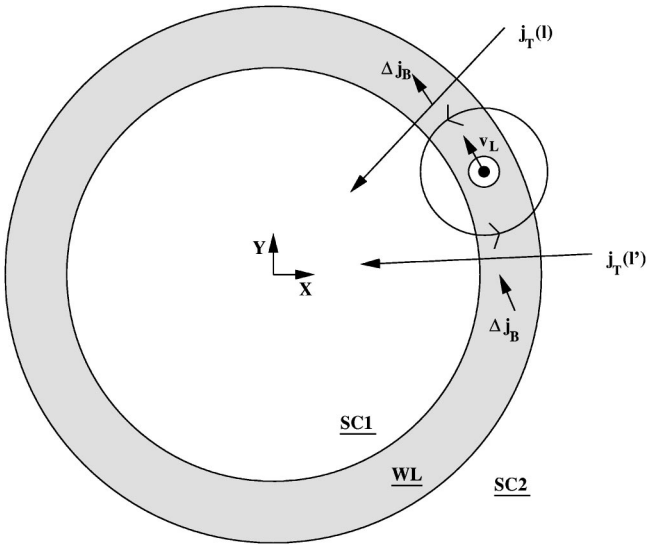

FIG. 3. Bias current density $\mathbf{j}_T(l)$ and the Berry-phase-induced current density $\Delta\mathbf{j}_B$ for a vortex moving in the $+\hat{\theta}$ direction. $\Delta\mathbf{j}_B$ points in the same direction as $\mathbf{v}_L$ since $\Delta\mathbf{j}_B=-\rho_s e\mathbf{v}_L$ and $e<0$. Note that $\Delta\mathbf{j}_B$ is drawn inside the weak link to make the figure easier to examine. Only the component of $\Delta\mathbf{j}_B$ normal to the local junction plane flows inside the weak link. The component of $\Delta\mathbf{j}_B$ parallel to the local junction plane flows inside the junction electrodes—it does *not* flow inside the weak link (see Sec. II A).

C. Nature of current drive modification

We have seen that Berry's phase leads to a modification of the current drive $\beta\rightarrow\beta'=\beta+\delta\beta(l,\tau)$. From Eq. (16) we see that $\delta\beta$ is proportional to the component of $\Delta\mathbf{j}_B$ along $\hat{\mathbf{r}}(l)$ (viz., normal to the local junction plane). We now show that $\delta\beta$ is spatially varying, and that for comparable situations, its spatial dependence for a vortex moving in the $+\hat{\theta}$ direction is exactly the opposite of what it is for a vortex moving in the $-\hat{\theta}$ direction.

In an AJJ, we note that the position of the vortex center and its antipodal point on the annular weak link divide the weak link into two half-circles. For a moving vortex, we will refer to the half-circle into which the vortex enters in the following instant as the region ''ahead'' of the vortex, while the other half-circle will be referred to as the region ''behind'' the vortex.

1. Vortex moving in the $+\hat{\theta}$ direction

In Fig. 3 we show a vortex with magnetic flux along $\hat{\mathbf{z}}$ moving in the $+\hat{\theta}$ direction. The bias current flows such that $\hat{\mathbf{j}}_T(l)=-\hat{\mathbf{r}}(l)$. One can show using either of the two heuristic approaches (Lorentz or Bernoulli) described in the Appendix that $\mathbf{j}_T$ does positive work on the vortex causing it to speed up. Let L be the circumference of the AJJ, so that $l=L(\theta/2\pi)$, and θ is the polar angle in the (r,θ) polar coordinate system detailed in Fig. 2. Then,

$$\hat{\mathbf{j}}_T(\theta)=-[\cos\theta\,\hat{\mathbf{x}}+\sin\theta\,\hat{\mathbf{y}}]. \tag{18}$$

If the vortex center is at $\theta'(\tau)$ at time τ, then

$$\dot{\mathbf{r}}_0(\tau)=v_L(\tau)[-\sin\theta'(\tau)\,\hat{\mathbf{x}}+\cos\theta'(\tau)\hat{\mathbf{y}}], \tag{19}$$

where $v_L(\tau)$ is the vortex speed at time τ. Plugging Eqs. (18) and (19) into Eq. (16) gives

$$\delta\beta(\theta,\tau)=\frac{\beta v_L(\tau)}{v_T}\sin[\theta'(\tau)-\theta]. \tag{20}$$

From Fig. 3 we see that the region ahead of the vortex corresponds to $\theta>\theta'(\tau)$ so that $\delta\beta<0$ ahead of the vortex. For the region behind the vortex, $\theta<\theta'(\tau)$, so that $\delta\beta>0$ behind the vortex. At the vortex center $[\theta=\theta'(\tau)]$ and at the center's antipode $[\theta=\theta'(\tau)+\pi]$, $\delta\beta=0$. Thus $\beta'=\beta+\delta\beta$ is reduced ahead of the vortex, enhanced behind it and unchanged at the vortex center and its antipode.

One can also arrive at these results for the spatial dependence of $\delta\beta$ by examining Fig. 3. Since the electric charge $e<0$, $\Delta\mathbf{j}_B=-\rho_s e\dot{\mathbf{r}}_0$ is parallel to the vortex velocity $\dot{\mathbf{r}}_0\equiv\mathbf{v}_L$. In this figure we draw $\Delta\mathbf{j}_B$ at a position ahead of, and behind, the vortex. To make the analysis which we are about to present easier to follow, we have drawn $\Delta\mathbf{j}_B$ inside the weak link. As is clear from the figure, $\Delta\mathbf{j}_B$ generally has components both normal and parallel to the local junction plane. As discussed in Sec. II A, the parallel component flows inside the junction electrodes as part of the surface supercurrents. It is vital that the reader be clear on this point: the parallel component of $\Delta\mathbf{j}_B$ does *not* flow inside the weak link—it flows inside the junction electrodes. On the other hand, the component of $\Delta\mathbf{j}_B$ normal to the local junction plane *does* flow inside the weak link. It contributes to the tunnel current density which continues to be everywhere normal to the local junction plane. The reader should not be misled by the way we have drawn $\Delta\mathbf{j}_B$ into thinking that the tunnel current density has a component parallel to the local junction plane; it does not.

Keeping these remarks about $\Delta\mathbf{j}_B$ in mind, Fig. 3 shows $\Delta\mathbf{j}_B$ at an arbitrary point ahead of the vortex, and we see that the normal projection of $\Delta\mathbf{j}_B$ is negative, $\Delta\mathbf{j}_B\cdot\hat{\mathbf{j}}_T(l)<0$, so that the effective current drive $\beta'=\beta+\delta\beta$ is reduced ahead of the vortex. Figure 3 also shows $\Delta\mathbf{j}_B$ at an arbitrary point behind the vortex. It is clear that the normal projection of $\Delta\mathbf{j}_B$ is positive at this point, $\Delta\mathbf{j}_B\cdot\hat{\mathbf{j}}_T(l')>0$, so that β' is enhanced behind the vortex. At the vortex center $\Delta\mathbf{j}_B$ and $\hat{\mathbf{j}}_T(l)$ are clearly perpendicular so that $\beta'=\beta$ at this point and also at its antipode. At the two points on the weak link midway between the vortex center and its antipode, $\Delta\mathbf{j}_B$ and $\hat{\mathbf{j}}_T$ are either parallel or antiparallel. Thus $|\delta\beta|$ is a maximum at these two points. This is in agreement with the above analysis based on Eq. (20).

2. Vortex moving in the $-\hat{\theta}$ direction

In Fig. 4 we show an AJJ containing the same vortex as in Fig. 3, only moving in the $-\hat{\theta}$ direction. Assume again that the vortex center is at $\theta'(\tau)$ and has speed $v_L(\tau)$ at time τ. To produce a situation comparable to that in Fig. 3 in which $\mathbf{j}_T$ does positive work on the vortex, we must have $\hat{\mathbf{j}}_T(l)=\hat{\mathbf{r}}(l)$. The argument leading up to Eq. (20) also works for

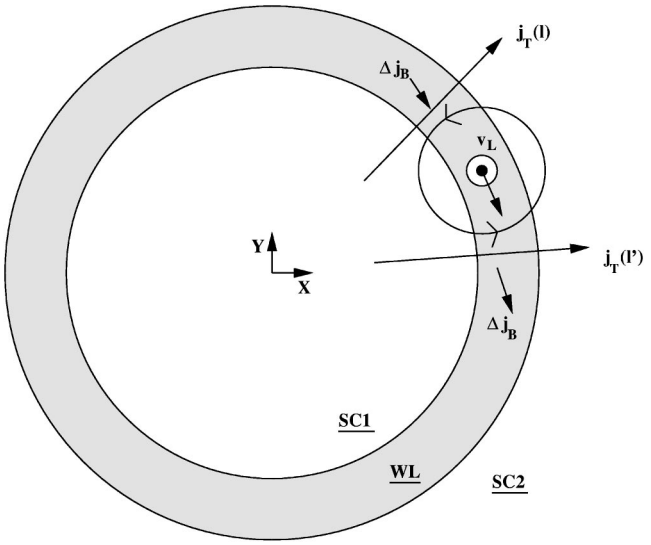

FIG. 4. Bias current density $\mathbf{j}_T(l)$ and the Berry-phase-induced current density $\Delta\mathbf{j}_B$ for a vortex moving in the $-\hat{\theta}$ direction. $\Delta\mathbf{j}_B$ points in the same direction as $\mathbf{v}_L$ since $\Delta\mathbf{j}_B=-\rho_s e\mathbf{v}_L$ and $e<0$. Note that $\Delta\mathbf{j}_B$ is drawn inside the weak link to make the figure easier to examine. Only the component of $\Delta\mathbf{j}_B$ normal to the local junction plane flows inside the weak link. The component of $\Delta\mathbf{j}_B$ parallel to the local junction plane flows inside the junction electrodes—it does *not* flow inside the weak link (see Sec. II A).

the present situation, though with $\dot{\mathbf{r}}_0\rightarrow-\dot{\mathbf{r}}_0$ and $\hat{\mathbf{j}}_T(\theta)\rightarrow-\hat{\mathbf{j}}_T(\theta)$, so that $\delta\beta(\theta,\tau)$ is again given by Eq. (20). Note that this time, however, the region ahead of the vortex corresponds to $\theta<\theta'(\tau)$ so that $\delta\beta>0$ ahead of the vortex. The region behind the vortex now corresponds to $\theta>\theta'(\tau)$ so that $\delta\beta<0$ behind the vortex. $\delta\beta$ again vanishes at the vortex center and at its antipode. Thus β' is enhanced ahead of the vortex, reduced behind the vortex, and unchanged at the vortex center and its antipode.

Figure 4 shows $\Delta\mathbf{j}_B$ at an arbitrary point ahead of, and behind, the vortex. The above remarks related to the drawing of $\Delta\mathbf{j}_B$ inside the weak link also apply to Fig. 4. From the figure we see that $\Delta\mathbf{j}_B\cdot\hat{\mathbf{j}}_T(l)$ is positive ahead of the vortex, negative behind it, and vanishes at the vortex center and its antipode. Thus the effective current drive β' is enhanced ahead of the vortex, reduced behind it, and uneffected at the vortex center and its antipode. $|\delta\beta|$ is again maximum at the two points midway between the vortex center and its antipode. This again agrees with the preceeding analysis based on Eq. (20).

We see that under comparable situations, the two directions of vortex motion produce current drive modifications $\delta\beta$ which are exact opposites of one another. This is a direct consequence of the sensitivity of Berry's phase to the vortex velocity $\dot{\mathbf{r}}_0$.

III. NECESSARY CONDITIONS FOR OBSERVABILITY

We have shown how Berry's phase leads to a modification $\delta\beta(l,\tau)$ of the current drive acting on a vortex at $T=0$:

$$\delta\beta(l,\tau)=\frac{\beta}{v_T}\hat{\mathbf{j}}_T(l)\cdot\dot{\mathbf{r}}_0(t). \tag{21}$$

Up to this point, besides requiring $T=0$, we have also required the weak link and electrodes to be in the clean limit and the weak link to be of uniform thickness. We now show that further restrictions are necessary if $\delta\beta$ is to be observable at finite temperature.

The first point to notice is the sensitivity of $\delta\beta$ to the geometrical arrangement of the superconducting electrodes in the AJJ. In particular, because of the scalar product $\hat{\mathbf{j}}_T(l)\cdot\dot{\mathbf{r}}_0(t)$ in Eq. (21), $\delta\beta(l,\tau)$ will vanish for a physically uninteresting reason if the geometrical arrangement of the electrodes constrains $\hat{\mathbf{j}}_T(l)$ to be everywhere perpendicular to $\dot{\mathbf{r}}_0(t)$. This situation occurs in the traditional linear Josephson junction and in the well-known Lyngby AJJ.[11]

(i) In the case of the linear Josephson junction, if we set up our coordinates so that the direction across the weak link $\hat{\mathbf{n}}=\hat{\mathbf{x}}$ and the magnetic flux of the vortex lies along $\hat{\mathbf{z}}$; then the junction geometry constrains the vortex to move along the y axis. Thus $\hat{\mathbf{j}}_T=\pm\hat{\mathbf{x}}$ and $\dot{\mathbf{r}}_0(t)=v_L(t)\hat{\mathbf{y}}$, and clearly $\hat{\mathbf{j}}_T\cdot\dot{\mathbf{r}}_0(t)=0$. Thus $\delta\beta=0$, and the current drive modification due to Berry's phase does not contribute to the dynamics of a linear Josephson junction.

(ii) For the Lyngby AJJ, the electrodes have an overlap structure so that $\hat{\mathbf{j}}_T(l)=\pm\hat{\mathbf{z}}$, while $\dot{\mathbf{r}}_0(t)$ is constrained to lie in the x-y plane. Thus $\delta\beta=0$ for all values of l, and it produces no effect in the dynamics of the Lyngby AJJ.

We see that if $\delta\beta$ is to produce observable consequences, we must restrict ourselves to AJJ's whose electrode arrangement ensures that $\hat{\mathbf{j}}_T(l)\cdot\dot{\mathbf{r}}_0(t)\neq0$ for some values of l. This requirement on the electrode arrangement defines the restricted class of AJJ's alluded to in Sec. II. Any attempt to observe $\delta\beta$ must be done using an AJJ belonging to this restricted class to insure that $\delta\beta$ does not vanish for trivial reasons. We now provide two examples of AJJ's which belong to this restricted class.

(i) In the planar AJJ shown in Figs. 1–4, $\hat{\mathbf{j}}_T(l)=\pm\hat{\mathbf{r}}(l)$ and $\dot{\mathbf{r}}_0(t)=(v_x(t),v_y(t),0)$ so that $\hat{\mathbf{j}}_T(l)\cdot\dot{\mathbf{r}}_0(t)\neq0$ at all points on the weak link except the vortex center and its antipode [see Eq. (20)]. Thus $\delta\beta(l,\tau)\neq0$ for this AJJ.

(ii) The cylindrical AJJ of Kuwada *et al.*[12] is another AJJ for which $\delta\beta(l,\tau)\neq0$. Here $\hat{\mathbf{j}}_T(l)=\pm\hat{\mathbf{r}}(l)$ and $\dot{\mathbf{r}}_0(t)=(v_x(t),v_y(t),0)$ so that $\delta\beta(l,\tau)$ is the same as for the planar AJJ.

Having defined the restricted class of AJJ's in which $\delta\beta(l,\tau)$ is not trivially quenched by a poor choice of electrode arrangement, we now examine the consequences of spectral flow for the observability of $\delta\beta$.

In the Appendix we show that in a clean superconducting film at $T=0$, Berry's phase produces a contribution to the nondissipative force $\mathbf{F}_{nd}$ acting on the vortex. Volovik[4] pointed out that the existence of quasiparticle states bound to the vortex core would strongly influence the observability of the Berry phase contribution to $\mathbf{F}_{nd}$. In the presence of nonzero temperature or impurity concentration, these levels are

broadened. When this broadening is roughly the same size as the interlevel energy spacing, Volovik argued that vortex motion would drive the levels adiabatically across the Fermi surface (spectral flow), producing excitations in the vortex core. In the hydrodynamic limit, this nonequilibrium population of the core states is quickly relaxed by interactions with the lattice, causing momentum to be transferred from the vortex core to the lattice. This spectral-flow-induced momentum transfer produces a force on the vortex which is found to be nearly equal and opposite to the Berry phase contribution to $\mathbf{F}_{nd}$.[4,5] Thus, in the hydrodynamic limit, the Berry phase contribution to $\mathbf{F}_{nd}$ is masked by spectral flow. Specifically, the linear momentum that enters the vortex core due to Berry phase processes is transferred to the lattice with nearly perfect efficiency by spectral flow so that the core retains effectively none of the momentum sent in by Berry's phase. In the collisionless limit, however, level broadening is negligible, relaxation processes are slow, and spectral flow does not occur.[3–5] If τ is the characteristic relaxation time for the core states and ΔE their characteristic energy-level spacing, then activation of spectral flow occurs when $\tau \sim \tau_* = \hbar/\Delta E$ so that the level broadening $\hbar/\tau$ is of order the level spacing ΔE. A clean superconductor at low temperature is in the collisionless limit so that spectral flow does not occur due to insufficient level broadening. Thus the Berry phase contribution to $\mathbf{F}_{nd}$ is not masked and can influence vortex motion. A dirty superconductor at sufficiently high temperature is in the hydrodynamic limit so that spectral flow is active and leads to a masking of the Berry phase contribution to $\mathbf{F}_{nd}$. Thus a crossover is expected in the dynamics of vortices when $\tau \sim \tau_*$: for $\tau \gg \tau_*$ (collisionless limit) there is no masking of Berry phase effects by spectral flow and $\mathbf{F}_{nd}$ has the Magnus force form (see the Appendix), while for $\tau \ll \tau_*$ (hydrodynamic limit) Berry phase effects are masked by spectral flow and $\mathbf{F}_{nd}$ has the Lorentz force form. This scenario is consistent with earlier work by Sonin[13] and by Kopnin and Kravtsov.[14]

Makhlin and Volovik[6] have argued that spectral flow similarly influences the observability of $\delta\beta(l,\tau)$ in an SNS AJJ. As in the case of a superconducting film, activation of spectral flow requires sufficient level broadening, only this time of quasiparticle states localized to the normal metal layer which acts as the weak link in the AJJ. For a *clean* SNS AJJ, spectral flow can only be activated thermally. As in the preceding discussion, at sufficiently low temperatures, spectral flow will not occur in a clean SNS AJJ, and $\delta\beta$ is observable. Above a crossover temperature T_*, spectral flow will occur, causing $\delta\beta$ to be masked and thus unable to influence vortex motion in the weak link. It is possible to crudely estimate the crossover temperature T_*. The quasiparticles localized on the weak link populate Landau levels with energy spacing $\Delta E = \hbar\omega_c$, where $\omega_c = eB/mc$ is the cyclotron frequency. The flux associated with the vortex, $\phi_0 = hc/2e$, is concentrated in a region of area $\lambda_J d$ so that $B = \phi_0/\lambda_J d$. The crossover is expected to occur when the thermal energy kT_* is of order ΔE so that

$$T_* \sim \frac{h^2}{4\pi m k \lambda_J d}. \tag{22}$$

Typically, $\lambda_J \sim 10^{-3}$ m and $d \sim 10^{-7}$ m so that $T_* \sim 0.1$ mK. It is important to remind the reader that this estimate is appropriate for a clean SNS AJJ. Note however that T_* decreases with increasing impurity concentration so that for sufficiently dirty junctions, $T_* = 0$. Having made this caveat about the importance of cleanliness, our estimate of T_* raises the hope that the crossover in the junction dynamics produced by activation of spectral flow at T_* might prove observable. Elsewhere,[15] we present the results of a numerical evaluation of the I-V characteristics for a planar SNS AJJ for $T \lesssim T_*$. In this temperature range $\delta\beta$ is small, but nonzero, and we examined the modifications that appear in the I-V curves as $\delta\beta$ is varied. We find that $\delta\beta$ (i) shifts the critical value of the bias current at which the AJJ switches and (ii) introduces lateral shifts in the vertical steps appearing in the I-V curves at large bias current. Both effects are found to be sensitive to the sense of vortex motion around the AJJ and provide a clear experimental signature of $\delta\beta$. These shifts are shown to be consequences of (1) the Berry phase modulation of the tunnel current density, (2) the appearance of a region of reversed magnetic flux at the trailing edge of the vortex core at large bias current in junctions with b-type dissipation [see Eq. (17)], and (3) Bernoulli's theorem. We refer the reader to Ref. 15 for a detailed presentation of these results.

IV. SUMMARY OF ESSENTIAL POINTS

In this paper we have shown in detail how Berry's phase leads to a modification $\delta\beta(l,\tau)$ of the current drive acting on a vortex in a restricted class of large AJJ's at sufficiently low temperature. $\delta\beta(l,\tau)$ was shown to be a consequence of a modulation of the tunnel current density flowing through the weak link caused by Berry's phase.[7]

We discussed at some length the circumstances which influence the observability of $\delta\beta$. The following restrictions were seen to be essential for a nonvanishing $\delta\beta$.

(i) To ensure that $\delta\beta$ is not trivially quenched, the geometrical arrangement of the electrodes in the AJJ must ensure that $\hat{\mathbf{j}}_T(l)\cdot\dot{\mathbf{r}}_0(t) \neq 0$ for some values of l. Two examples were presented of AJJ's that satisfy this condition.

(ii) To ensure that spectral flow does not mask $\delta\beta$, it is necessary that the electrodes and weak link be in the clean limit and the temperature be safely below the crossover temperature T_* at which spectral flow can be thermally activated.

(iii) To ensure that the vortex is not pinned or scattered by inhomogeneities in the thickness of the weak link, the weak link is required to be of uniform thickness. Such inhomogeneities are expected to predominantly influence the junction dynamics at small bias currents. They will be less significant at larger bias currents which are sufficiently energetic to depin the vortex.

In a separate paper,[15] we examine numerically the consequences of $\delta\beta$ on the I-V characteristics of a planar SNS AJJ for $T \lesssim T_*$. We find clear experimental signatures of $\delta\beta$ in the I-V curves, and provide an explanation of the physics underlying these Berry phase effects.

ACKNOWLEDGMENTS

I would like to thank T. Howell III for continued support and Subodh Shenoy for encouragement.

APPENDIX: BERRY'S PHASE AND VORTICES IN A TWO-DIMENSIONAL SUPERCONDUCTOR

In this appendix we summarize the argument which indicates that, under appropriate restrictions (see below), Berry's phase will cause a modification of the superflow associated with a transport current that flows past a moving vortex in a superconducting thin film. We then relate this superflow modification to the nondissipative force acting on the vortex. For a more detailed presentation, the reader is referred to Ref. 16. This flow modification is the origin of the current drive modification discussed at length in Sec. II. It is worth pointing out that Ref. 16 explicitly assumed $T=0$ and a vanishing impurity potential. Consequently, the conclusion reached there regarding the Berry phase contribution to the nondissipative force only applies in the low-temperature, clean limit. As discussed in Sec. III, at sufficiently high temperature and/or impurity concentration, spectral flow produces a masking of this Berry phase contribution to the nondissipative force.[4,5] The original realization that Berry's phase can influence vortex motion in a superconductor is due to Ao and Thouless.[17]

We begin by restricting the following analysis to an *s*-wave superconducting thin film. The dynamics of the Bogoliubov quasiparticles (BQP's) is governed by the Bogoliubov Hamiltonian $H_B[\mathbf{r}_0]$:

$$H_B[\mathbf{r}_0]=\begin{pmatrix} \frac{1}{2m}\left(-i\hbar\nabla-\frac{e}{c}\mathbf{A}\right)^2-E_f+U_0(\mathbf{r}) & \Delta(\mathbf{r}-\mathbf{r}_0) \\ \Delta^*(\mathbf{r}-\mathbf{r}_0) & -\frac{1}{2m}\left(i\hbar\nabla-\frac{e}{c}\mathbf{A}\right)^2+E_f-U_0(\mathbf{r}) \end{pmatrix}.$$

Here $\mathbf{A}$ is the vector potential associated with the magnetic field $\mathbf{H}$, and E_f is the Fermi energy. $U_0(\mathbf{r})$ is the impurity potential which we assume vanishes so that we are limiting ourselves to the case of a clean superconducting film. Later we will further restrict ourselves to $T=0$. Here $\Delta(\mathbf{r}-\mathbf{r}_0)$ is the superconducting gap function, and $\mathbf{r}_0$ marks the location of a vortex in the superconducting thin film. For this case, the gap function takes the form $\Delta(\mathbf{r}-\mathbf{r}_0)=\Delta_0(|\mathbf{r}-\mathbf{r}_0|)\exp[-i\theta(\mathbf{r}-\mathbf{r}_0)]$. The gap amplitude Δ_0 vanishes at the vortex center ($\mathbf{r}=\mathbf{r}_0$), and reaches its bulk value within a coherence length of the vortex center. The gap phase $\phi=-\theta(\mathbf{r}-\mathbf{r}_0)$ is (to within a sign) the azimuthal angle $\theta(\mathbf{r}-\mathbf{r}_0)$ of $\mathbf{r}$ relative to $\mathbf{r}_0$. Consequently, ϕ is not single valued, but changes by 2π as $\mathbf{r}$ winds around $\mathbf{r}_0$.

For a stationary vortex, the eigenfunctions $\chi_n(\mathbf{r}-\mathbf{r}_0)$ of $H_B[\mathbf{r}_0]$ depend explicitly on $\mathbf{r}_0$:

$$\chi_n(\mathbf{r}-\mathbf{r}_0)=\begin{pmatrix} u_n(\mathbf{r}-\mathbf{r}_0) \\ v_n(\mathbf{r}-\mathbf{r}_0) \end{pmatrix}.$$

The creation operator $\gamma_{n\downarrow}$ for an energy eigenstate with $E_n<E_f$ is

$$\gamma_{n\downarrow}=\int d^3x[-\psi_\uparrow^\dagger(\mathbf{r})v_n^*(\mathbf{r}-\mathbf{r}_0)+\psi_\downarrow(\mathbf{r})u_n^*(\mathbf{r}-\mathbf{r}_0)], \tag{A1}$$

where $\psi_s(\mathbf{r}-\mathbf{r}_0)$ ($s=\uparrow,\downarrow$) are the field operators for the Landau quasiparticles. [Note that, although we are considering a thin film, we include the (passive) height dimension of the film in the integration measure d^3x. This ensures that we do not overlook the height contribution to the dimensional analysis of $\overline{S_{cd}}$ given in Sec. II B.] The BCS ground state is formed by occupying all energy eigenstates with $E_n<E_f$:

$$|\mathrm{BCS}\rangle_{\mathbf{r}_0}=\prod_n \gamma_{n\downarrow}|0\rangle. \tag{A2}$$

The subscript on the BCS ground state indicates that the vortex is located at $\mathbf{r}_0$.

For a moving vortex, the vortex trajectory $\mathbf{r}_0(t)$ causes the Bogoliubov Hamiltonian to become time dependent: $H_B[\mathbf{r}_0(t)]$. Typically, vortex motion is sufficiently slow that this time dependence can be considered adiabatic.[18] Explicit calculation[16] shows that a Berry phase ϕ_n (not to be confused with the gap phase ϕ) is generated in the instantaneous energy eigenstates: $(u_n v_n)\rightarrow\exp[i\phi_n](u_n v_n)$. From Eq. (A1), this causes $\gamma_{n\downarrow}$ to inherit (minus) this phase: $\gamma_{n\downarrow}\rightarrow\exp[-i\phi_n]\gamma_{n\downarrow}$. Consequently, from Eq. (A2), the BCS ground state develops a Berry phase Γ:

$$|\mathrm{BCS}\rangle\rightarrow\exp[i\Gamma]|\mathrm{BCS}\rangle_{\mathbf{r}_0(t)}, \tag{A3}$$

where,

$$\Gamma=-\sum_n \phi_n.$$

Explicit calculation give

$$\Gamma=-\int dt\, d^3x\, \rho_s\left[\frac{1}{2}\partial_t\gamma+\frac{e}{\hbar}\xi\right]. \tag{A4}$$

Here $\gamma=\phi-(2e/\hbar c)\int^{\mathbf{x}}d\mathbf{l}\cdot\mathbf{A}$ is the gauge-invariant gap phase, and $\xi=-\int^{\mathbf{x}}d\mathbf{l}\cdot\mathbf{E}=A_0+(1/c)\int^{\mathbf{x}}d\mathbf{l}\cdot\mathbf{A}$ is the emf. ρ_s is the $T=0$ superfluid density, and it has arisen because we

have focused on the BCS ground state. Consequently, Γ can only depend on the $T=0$ properties of the superconductor. It is because our calculations are based on the BCS ground state that our results are restricted to $T=0$ as mentioned earlier. It is a simple matter to show that $(\hbar/2)\partial_t\gamma+e\xi=(\hbar/2)\partial_t\phi+eA_0$ so that Eq. (A4) agrees with Eq. (20) of Ref. 16.

To see how Berry's phase is able to influence the dynamics of the BQP's, we examine the condensate effective action S:

$$\exp\left[\frac{i}{\hbar}S\right]={}_{\mathbf{r}_0(T)}\langle \mathrm{BCS}|U(T,0)|\mathrm{BCS}\rangle_{\mathbf{r}_0(0)}.$$

Note that because S is defined in terms of the ground-state-to-ground-state transition amplitude, we are again explicitly restricting our results to $T=0$. Because of the adiabatic time dependence, $U(T,0)$ propagates $|\mathrm{BCS}\rangle_{\mathbf{r}_0(0)}$ into $|\mathrm{BCS}\rangle_{\mathbf{r}_0(T)}$ to within a phase factor which is fixed by the quantum adiabatic theorem[2]

$$U(T,0)|\mathrm{BCS}\rangle_{\mathbf{r}_0(0)}=\exp\left[i\Gamma-\frac{i}{\hbar}\int_0^T dt\,E_0(t)\right]|\mathrm{BCS}\rangle_{\mathbf{r}_0(T)}. \tag{A5}$$

Projecting Eq. (A5) onto $|\mathrm{BCS}\rangle_{\mathbf{r}_0(T)}$ yields the effective action S:[16]

$$\begin{aligned}S&=\hbar\Gamma+S_2\\&=\int dt\,d^3x\left[-\rho_s\left(\frac{\hbar}{2}\partial_t\gamma+e\xi\right)-\frac{m\rho_s}{2}\mathbf{v}_s^2\right.\\&\quad\left.+N(0)\left(\frac{\hbar}{2}\partial_t\gamma+e\xi\right)^2+\frac{1}{8\pi}\{(\mathbf{H}-\mathbf{H}_{ext})^2-\mathbf{E}^2\}\right].\end{aligned} \tag{A6}$$

Here $\mathbf{v}_s(\mathbf{r})$ is the velocity field associated with the superflow present in the superconducting film, and $N(0)$ is the single-particle density of states evaluated at the Fermi energy. $\mathbf{H}_{ext}$ is the externally applied magnetic field, $\mathbf{H}$ is the local magnetic field, and $\mathbf{E}$ is the electric field produced by the moving vortex. We see that the Berry phase Γ now appears in the condensate effective action S and is thus able to influence the condensate dynamics. The first term in the square brackets is the Berry phase contribution to the condensate's effective Lagrangian. That Berry's phase can enter as a term in a low-energy effective Lagrangian is well known;[19] such a term is known as a Wess-Zumino term.

Imagine now that a transport current $\mathbf{j}_T=\rho_s e\mathbf{v}_T$ is passed through our superconducting film. This current adds to the screening current $\mathbf{j}_{circ}=\rho_s e\mathbf{v}_{circ}$ which circulates around the vortex core, and here $\mathbf{v}_{circ}=(\hbar/2m)\nabla\gamma$. Thus, the total velocity field is $\mathbf{v}_s=\mathbf{v}_T+\mathbf{v}_{circ}$. This corresponds to the physical situation encountered in a Hall effect experiment.

The terms in S which are linear in $\nabla_{\mathbf{r}}\gamma$ determine the driving force which acts on the vortex. (This force is distinct from dissipative or pinning forces which may also act on the vortex.) Two such terms appear in S. The first appears in the Berry phase contribution to S. This follows since $\gamma=\gamma(\mathbf{r}-\mathbf{r}_0(t))$ so that $\partial_t\gamma=-\dot{\mathbf{r}}_0\cdot\nabla_{\mathbf{r}}\gamma$. The second appears in the stiffness term $-m\rho_s\mathbf{v}_s^2/2$. In fact, since $\mathbf{v}_s^2=(\mathbf{v}_T+\mathbf{v}_{circ})^2$, the cross term $2\mathbf{v}_T\cdot\mathbf{v}_{circ}$ gives rise to the second term of interest: $-(\rho_s\hbar/2)\mathbf{v}_T\cdot\nabla_{\mathbf{r}}\gamma$. Thus the action associated with the vortex drive is

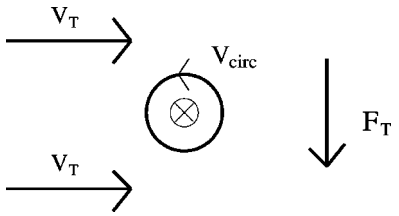

FIG. 5. Hydrodynamic force $\mathbf{F}_T$ acting on a vortex with magnetic flux pointing into the page due to a superflow $\mathbf{v}_T$. The screening currents produce a superflow $\mathbf{v}_{circ}$ which circulates counterclockwise around the vortex core.

$$\begin{aligned}S_{dr}&=\int dt\,d^3x\left[-\frac{\rho_s\hbar}{2}(\mathbf{v}_T-\dot{\mathbf{r}}_0)\cdot\nabla_{\mathbf{r}}\gamma\right]\\&=\int dt\,d^3x\left(-\frac{\hbar}{2e}\right)(\rho_s e\mathbf{v}_T-\rho_s e\dot{\mathbf{r}}_0)\cdot\nabla_{\mathbf{r}}\gamma\\&=\int dt\,d^3x\left(-\frac{\hbar}{2e}\right)(\mathbf{j}_T+\Delta\mathbf{j}_B)\cdot\nabla_{\mathbf{r}}\gamma.\end{aligned} \tag{A7}$$

We see that the ground-state Berry phase Γ has led to a modification of the current density which couples to the vortex: $\mathbf{j}_T\rightarrow\mathbf{j}_T+\Delta\mathbf{j}_B$, where $\Delta\mathbf{j}_B=-\rho_s e\dot{\mathbf{r}}_0$. Note that since $e<0$, $\Delta\mathbf{j}_B$ is parallel to the vortex velocity $\dot{\mathbf{r}}_0$. In Ref. 16 it was shown that S_{dr} causes the (nondissipative) driving force $\mathbf{F}_{nd}$ to act on the vortex:

$$\mathbf{F}_{nd}=\frac{\rho_s h}{2}(\mathbf{v}_T-\dot{\mathbf{r}}_0)\times\hat{\mathbf{z}}. \tag{A8}$$

Thus, for a clean superconducting film at $T=0$, the nondissipative driving force acting on a vortex has the Magnus force form with the contribution proportional to $\dot{\mathbf{r}}_0\times\hat{\mathbf{z}}$ having its origin in the BCS ground-state Berry phase Γ. As discussed in Sec. III, the Berry phase contribution to $\mathbf{F}_{nd}$ is masked by spectral flow effects at sufficiently high temperature and/or impurity concentration.[4,5]

We close by presenting two heuristic analyses of the $T=0$ clean limit form of $\mathbf{F}_{nd}$ which we have found instructive.

(1) We rewrite Eq. (A8) as

$$\mathbf{F}_{nd}=\frac{1}{c}(\rho_s e\mathbf{v}_T-\rho_s e\dot{\mathbf{r}}_0)\times\left(-\frac{hc}{2|e|}\hat{\mathbf{z}}\right)=\frac{1}{c}\mathbf{j}\times\mathbf{\Phi}, \tag{A9}$$

where $\mathbf{j}=\mathbf{j}_T+\Delta\mathbf{j}_B$, and $\mathbf{\Phi}$ is the magnetic flux associated with the vortex. Thus one can consider $\mathbf{F}_{nd}$ as the Lorentz force acting on the vortex, although the current density $\mathbf{j}$ which couples to the moving vortex contains a Berry-phase-induced modification $\Delta\mathbf{j}_B=-\rho_s e\dot{\mathbf{r}}_0$.

(2) In Fig. 5 we show the superflow $\mathbf{v}_T$ associated with the transport current $\mathbf{j}_T$. The magnetic flux of the vortex points into the page so that the screening superflow $\mathbf{v}_{circ}$ circulates counterclockwise ($\mathbf{j}_{circ}$ flows clockwise). It is clear from the

figure that the transport flow $\mathbf{v}_T$ enhances the circulating flow $\mathbf{v}_{circ}$ below the vortex and reduces it above. Thus, by Bernoulli's law, the transport current produces a hydrodynamic force $\mathbf{F}_T$ acting downward on the vortex. Formally, this force is given by the Kutta-Joukowski force so that $\mathbf{F}_T = m\rho_s \mathbf{v}_T \times \mathbf{\Gamma} = (\rho_s h/2)\mathbf{v}_T \times \hat{\mathbf{z}}$, where $\mathbf{\Gamma} = (h/2m)\hat{\mathbf{z}}$ is the circulation associated with the vortex (not to be confused with the ground-state Berry phase Γ). In Fig. 6, $\dot{\mathbf{r}}_0$ is the vortex velocity, and the Berry phase modification of the flow velocity, $\Delta\mathbf{v}_B = \Delta\mathbf{j}_B/\rho_s e = -\dot{\mathbf{r}}_0$, is shown passing the same vortex that appears in Fig. 5. A Bernoulli analysis of the situation depicted in Fig. 6 shows that a hydrodynamic force $\mathbf{F}_B$ acts on the vortex due to the Berry phase modification of the superflow $\Delta\mathbf{v}_B$. The direction of $\mathbf{F}_B$ is shown in Fig. 6, and here the Kutta-Joukowski force is $\mathbf{F}_B = m\rho_s(-\dot{\mathbf{r}}_0) \times \mathbf{\Gamma} = -(\rho_s h/2)\dot{\mathbf{r}}_0 \times \hat{\mathbf{z}}$. Thus the total hydrodynamic force $\mathbf{F}_{hyd}$ is the sum of $\mathbf{F}_T$ and $\mathbf{F}_B$,

$$\mathbf{F}_{hyd} = \frac{\rho_s h}{2}(\mathbf{v}_T - \dot{\mathbf{r}}_0) \times \hat{\mathbf{z}}, \tag{A10}$$

reproducing the vortex driving force in Eq. (A8).

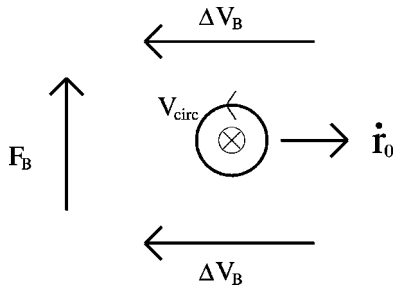

FIG. 6. Hydrodynamic force $\mathbf{F}_B$ acting on a vortex with magnetic flux pointing into the page due to the Berry phase modification of the superflow $\Delta\mathbf{v}_B = -\dot{\mathbf{r}}_0$, where $\dot{\mathbf{r}}_0$ is the vortex velocity. The screening currents produce a superflow $\mathbf{v}_{circ}$ which circulates counterclockwise around the vortex core.

In both of these heuristic analyses, it is the Berry phase modification of the superflow passing over the vortex $\Delta\mathbf{j}_B$ that gives rise to the portion of $\mathbf{F}_{nd}$ which is proportional to $\dot{\mathbf{r}}_0 \times \hat{\mathbf{z}}$. As shown in Sec. II, $\Delta\mathbf{j}_B$ is the origin of the Berry phase modification of the current drive acting on a vortex in a restricted class of large annular Josephson junction at $T = 0$. As discussed in Sec. III, at sufficiently high temperatures, this Berry phase effect is masked by spectral flow.

*Electronic address: gaitan@physics.siu.edu

[1] F. Gaitan and S.R. Shenoy, Phys. Rev. Lett. **76**, 4404 (1996).
[2] M.V. Berry, Proc. R. Soc. London, Ser. A **392**, 45 (1984).
[3] N.B. Kopnin, G.E. Volovik, and Ü. Parts, Europhys. Lett. **32**, 651 (1995).
[4] G.E. Volovik, Zh. Éksp. Teor. Fiz. **104**, 3070 (1993) [Sov. Phys. JETP **77**, 435 (1993)].
[5] M. Stone, Phys. Rev. B **54**, 13 222 (1996).
[6] Y.G. Makhlin and G.E. Volovik, Pis'ma Zh. Éksp. Teor. Fiz. **62**, 923 (1995) [JETP Lett. **62**, 941 (1995)].
[7] Berry's phase also modifies the supercurrents flowing parallel to the surface of the junction electrodes, although this effect is not relevant to the current drive modification that is the subject of this paper. For further discussion, see Sec. II A and II C.
[8] B.D. Josephson, Adv. Phys. **14**, 419 (1965).
[9] D.W. McLaughlin and A.C. Scott, Phys. Rev. A **18**, 1652 (1978).
[10] A. C. Scott, *Active and Nonlinear Wave Propogation in Electronics* (Wiley-Interscience, New York, 1970).
[11] A.V. Ustinov, T. Doderer, R.P. Huebener, N.F. Pedersen, B. Mayer, and V.A. Oboznov, Phys. Rev. Lett. **69**, 1815 (1992).
[12] M. Kuwada, Y. Onodera, and Y. Sawada, Phys. Rev. B **27**, 5486 (1983).
[13] E.B. Sonin, Rev. Mod. Phys. **59**, 87 (1987).
[14] N.B. Kopnin and V.E. Kravtsov, Zh. Éksp. Teor. Fiz. **71**, 1644 (1976) [Sov. Phys. JETP **44**, 861 (1976)].
[15] V. Plerou and F. Gaitan, following paper, Phys. Rev. B **63**, 104512 (2001).
[16] F. Gaitan, Phys. Rev. B **51**, 9061 (1995).
[17] P. Ao and D.J. Thouless, Phys. Rev. Lett. **70**, 2158 (1993).
[18] J. Bardeen, Phys. Rev. Lett. **13**, 747 (1964).
[19] A. Shapere and F. Wilczek, *Geometric Phases in Physics* (World Scientific, Singapore, 1989), Chap. 7.